

Published in final edited form as:

J Biomed Mater Res A. 2010 January ; 92(1): 18–32. doi:10.1002/jbm.a.32279.

A bovine acellular scaffold for vocal fold reconstruction in a rat model

Chet C. Xu¹, Roger W. Chan^{1,2,*}, Debra G. Weinberger¹, Guy Efuno¹, and Karen S. Pawlowski¹

¹ Otolaryngology – Head and Neck Surgery, University of Texas Southwestern Medical Center

² Biomedical Engineering, University of Texas Southwestern Medical Center

Abstract

With a rat model of vocal fold injury, this study examined the *in vivo* host response to an acellular xenogeneic scaffold derived from the bovine vocal fold lamina propria, and the potential of the scaffold for constructive tissue remodeling. Bilateral wounds were created in the posterior vocal folds of 20 rats, and bovine acellular scaffolds were implanted into the wounds unilaterally, with the contralateral vocal folds as control. The rats were humanely sacrificed after 3 days, 7 days, 1 month, and 3 months, and the coronal sections of their larynges were examined histologically. Expressions of key matrix proteins including collagen I, collagen III, elastin, fibronectin, hyaluronic acid, and glycosaminoglycans were quantified with digital image analysis. Significant infiltration of host inflammatory cells and host fibroblasts in the scaffold implant was observed in the acute stage of wound repair (3 days and 7 days post-surgery). The mean relative densities of collagen I, collagen III, and glycosaminoglycans in the implanted vocal folds were significantly higher than those in the control after 3 days, followed by gradual decreases over 3 months. Histological results showed that the scaffolds were apparently degraded by 3 months, with no fibrotic tissue formation or calcification. These preliminary findings suggested that the bovine acellular scaffold could be a potential xenograft for vocal fold regeneration.

Keywords

biocompatibility; extracellular matrix scaffold; foreign body response; larynx; xenotransplantation

INTRODUCTION

An estimated 3–9% of Americans suffer from some kind of voice disorders every year, 1 causing adverse impact on phonation (voice production), communication, and the quality of life of these individuals. Only very limited medical and surgical options are available for treating laryngeal pathologies characterized by tissue damage and deficiencies in the vocal fold lamina propria, such as vocal fold scarring, sulcus vocalis, and vocal fold atrophy. 2 One of the primary reasons for this limitation is that an optimal, surgically implantable biomaterial for reconstruction of the vocal fold extracellular matrix (ECM) has yet to be developed. Such a material should have biomechanical properties and vibratory properties similar to those of the vocal fold ECM, so that normal or near-normal acoustical characteristics of phonation and perceptual voice quality can be achieved. The implantable

#No benefit of any kind will be received either directly or indirectly by the authors.

*Corresponding author: Roger W. Chan, Otolaryngology – Head and Neck Surgery, University of Texas Southwestern Medical Center, 5323 Harry Hines Blvd., Dallas, TX 75390-9035, U. S. A. Phone: (214) 648-0386 FAX: (214) 648-9122, Email: roger.chan@utsouthwestern.edu.

material must also simulate the complex composition of the vocal fold ECM given the crucial contributions of various matrix proteins to the homeostasis of cells in the vocal fold lamina propria, such as fibroblasts, myofibroblasts, macrophages, and stellate cells. 3–5 In addition, in order to restore any impaired vocal fold geometry, the material should also provide relatively long-lasting augmentation while allowing for new tissue formation and constructive remodeling.

We have recently developed a bovine acellular, xenogeneic scaffold for vocal fold tissue engineering. 6 It was found to hold promise because its biomechanical properties were close to those of the human vocal fold lamina propria, it was biocompatible with human primary-culture vocal fold fibroblasts *in vitro*, and also because it demonstrated a set of pore properties favorable for cellular attachment, infiltration, and the transport of biofactors. 7 In the present study, a rat model of vocal fold injury was used to assess the biocompatibility of the acellular scaffold, in terms of the *in vivo* host response and host tissue remodeling, the scaffold degradation, and its potential for tissue reconstruction. The rat model has been widely used for vocal fold studies due to the vocal communication nature of rats, 8 as well as the histological similarities between the rat and the human vocal fold. 9 It has also been reported that rats can vocalize over a wide range of frequencies in the audible range and in the ultrasonic range, up to about 50 kHz, 10 whereas the frequencies of human phonation range from around 100Hz to 1000Hz. 11 Bovine acellular scaffolds were implanted unilaterally into surgically created vocal fold wounds, with the contralateral vocal folds as control. At different time points following the implantation, the larynx of each animal was harvested and examined histologically, so as to evaluate the host response to the scaffold.

MATERIALS AND METHODS

Fabrication of bovine acellular scaffolds

Bovine acellular scaffolds were fabricated from native bovine vocal fold lamina propria specimens, using a saline-based osmotic decellularization approach. 6 Four bovine larynges were harvested from heifers and bulls (approximately 30 months old; body weight ranging from about 273–591 kg) from a local abattoir. The animal euthanization protocol was approved by the U.S. Department of Agriculture Meat and Poultry Inspection Program. In each larynx, the lamina propria was dissected from each vocal fold using phonomicrosurgical instruments, followed by mounting on a custom-built plastic frame to sustain an *in situ* tissue tension. Briefly, the decellularization protocol involved sequential incubation of the mounted lamina propria specimens in 3M sodium chloride solution, isotonic phosphate-buffered saline (PBS) solution with DNase and RNase, and 75% ethanol. 6 75% instead of 70% ethanol (as in Xu et al. 6) was used because it was found that the decellularization was more complete with minimal disruption of the matrix proteins in the scaffolds. Each decellularized scaffold was cut into a near-rectangular shape of around 1.5mm by 0.5mm, with a native thickness of around 0.5–0.75mm, and was stored in sterilized PBS solution at 4°C. Most acellular scaffolds were implanted into the animals within one week, and all were implanted within 20 days of the fabrication. Just prior to the experiments with rats, the acellular scaffolds were sterilized again using 70% ethanol and UV light, the same sterilization method as in previous *in vitro* cell culture studies because it was found effective in preventing microbial contaminations. 6

Animal surgery

Twenty one adult male Sprague-Dawley rats, each with body weight from around 400g to 500g, were procured from the Charles River Laboratories, Inc. (Wilmington, MA). One of these rats was used to examine the effect of the surgical procedure on the vocal fold, whereas the other twenty served as the experimental rats. The rats were housed in separate

cages at 25°C. Daily records of eating, drinking, general behavior and appearance were maintained. All experimental procedures were approved by the Institutional Animal Care and Use Committee (IACUC) of UT Southwestern Medical Center (approval date: March 7, 2007), in accordance with the U.S. Public Health Service Policy on Humane Care and Use of Laboratory Animals, the NIH Guide for the Care and Use of Laboratory Animals (NIH Publication #85-23 Rev. 1985), and the Animal Welfare Act (7 U.S.C. et seq.).

The rats were anesthetized with inhalation of 4% isoflurane followed by an intraperitoneal injection of ketamine (Ketaset, 65 mg/kg body weight) (Fort Dodge Animal Health, Fort Dodge, IA) and xylazine (X-ject SA, 6.5 mg/kg body weight) (Butler Animal Health Supply, Dublin, OH). Carprofen (Rimadyl, 5.0 mg/kg body weight) (Pfizer Animal Health, New York, NY) was also given subcutaneously to minimize any possible swelling of the vocal folds during surgery. Figure 1 illustrates the surgical procedure. The anesthetized animal was placed on a customized operating platform in supine position (Figure 1A). An otoscope specula with a 4-mm orifice (Welch Allyn Inc., Skaneateles Falls, NY) was secured in the oral cavity to allow for the insertion of phonomicrosurgical instruments, and to allow for visualization of the vocal folds through a surgical microscope (M655, Leica Microsystems Inc., Bannockburn, IL) (Figs. 1B and 1C). To reduce respiratory movement of the vocal folds for facilitating the surgical procedure, about 100 µl of a topical anesthesia, 2% lidocaine (Lidoject, Butler Animal Health Supply, Dublin, OH), was applied to the surface of the vocal folds using a 100 µl pipet.

Figure 2 shows the anatomy of the rat larynx schematically as seen from a superior view, similar to that of Figure 1C. In the larynx of each experimental rat, a wound site was surgically created on the superior surface of the posterior one-third of each vocal fold, approximately 0.8 mm lateral to the vocal fold free edge. For each wound, a 1-mm long longitudinal incision was made to a depth of about 0.5mm to 2.0mm with a customized cutting tool derived from the stylet of an 18-gauge spinal needle. Microforceps were used to deliver the bovine acellular scaffolds into the wounds unilaterally, with the contralateral vocal folds as control. No suturing or surgical glue (e.g., fibrin glue) was required to affix the scaffolds or close the wounds, as each scaffold was secured in the implant site by the geometric difference between the scaffold and the wound (with the scaffold being larger than the incision). A similar implantation approach has been reported in a rabbit model of the vocal fold.¹² In the rat for examining the effect of the surgical procedure (Figure 1D), the wound was only created on the left vocal fold, with the right vocal fold intact as a control. Minimal bleeding and swelling could be seen immediately following the surgery (Figure 1D). After 24 hours, the vocal fold with an implanted scaffold was observed to be normal in gross structure (Figure 1E). During the surgery, oxygen was provided to ensure a sufficient level of oxygen saturation. Heart rate and oxygen saturation of the rats were closely monitored by a veterinarian vital signs monitor (SurgiVet V9200, Smiths Medical PM, Waukesha, WI).

After surgery, the rats were placed on a heating pad and were provided with oxygen. When their oxygen saturation became steady and reached a level above 95%, the rats were returned to illuminated warm cages for further recovery. All rats were monitored until they were able to ambulate, upon which they were returned to the housing facility. Antibiotics were provided to the animals given that the surgery was conducted in the non-sterilized airway. Also, a soft diet Nutra-Gel (Bio-Serv, Frenchtown, NJ) mixed with sulfamethoxazole/trimethoprim (Hi-Tech Pharmacal Co., Amityville, NY) was given to the rats in the first three days following surgery, in order to facilitate their recovery as well as to prevent any possible infection.

On day 3, day 7, day 30 and day 90 (five rats for each time point), the rats were humanely euthanized by an intraperitoneal injection of Euthasol (Virbac AH, Fort Worth, TX), a 390mg pentobarbital sodium / 50mg phenytoin sodium per ml solution. Monitoring of each animal continued until the absence of a heart beat. Immediately following euthanasia, the larynges were excised and stored in 10% formalin for further histological processing and examination.

Histological examination with hematoxylin and eosin (H&E) and Alcian blue

The host response to the implanted scaffold was examined histologically by hematoxylin and eosin (H&E). The rat larynges were fixed overnight in 10% formalin immediately following harvest, and were embedded in paraffin for sectioning. Successive 5.0 μm -thick coronal sections of the laryngeal specimens were prepared with a microtome (RM 2255, Leica Microsystems Inc., Bannockburn, IL), and mounted on glass slides. The slide sections were deparaffinized with xylene and were gradually rehydrated in 100% ethanol, 95% ethanol, 70% ethanol and distilled water. After that, deparaffinized sections were stained by Harris hematoxylin solution (Sigma, St. Louis, MO), followed by washes in tap water, 70% ethanol with 1.0% hydrochloric acid, Scott's solution (0.2% ammonium hydroxide solution), and 95% ethanol. The sections were then counter-stained with eosin Y solution (Sigma, St. Louis, MO). Cover-slips were applied to the stained sections after they were dehydrated with 95% ethanol and 100% ethanol, and cleared with xylene.

Glycosaminoglycans (GAGs) synthesized by the host fibroblasts as well as those inherent in the bovine acellular scaffold were visualized by Alcian blue staining since the Alcian blue dye binds in proportion to the number of negative charges on the side chains of the GAG molecules.^{13, 14} In brief, deparaffinized sections of the laryngeal specimens were incubated in 1.0% Alcian blue staining solution (1.0% Alcian blue 8GX in 3.0% acetic acid solution, pH = 2.5) for 30 min. at room temperature, followed by washing in tap water for 2 min., and rinsing in distilled water for 5 min. Cover-slips were applied to the stained sections.

Immunohistochemical examination

The immunohistochemical examination focused on the matrix proteins collagen I, collagen III, elastin, fibronectin, and hyaluronic acid (HA), since they have been identified as key contributors to cellular homeostasis and ECM remodeling in the vocal fold.^{3, 4, 6} Table 1 shows the antibodies used to visualize collagen I, collagen III, elastin, fibronectin, and HA. The antibodies (except for HA, as described below) were carefully selected and tested in a preliminary study to ensure that they specifically targeted rat proteins without positively staining the bovine acellular scaffold. Figure 3 illustrates the histological results involving the anti-rat fibronectin antibody, where a rat laryngeal coronal section implanted with a bovine acellular scaffold (Fig. 3A) and an acellular scaffold sample alone (Fig. 3B) were subjected to the same immunohistochemical staining procedure described next. Identical microscopic settings were used, and the same image acquisition procedure was followed. Similar to the results shown in Fig. 3, all four antibodies were found to specifically target the rat proteins, rather than those of the implanted bovine acellular scaffolds.

To prepare for immunohistochemical staining, 5.0 μm paraffin sections of the laryngeal specimens were deparaffinized in xylene, and gradually hydrated in a series of 100%, 95%, 70%, 50%, and 30% ethanol. In order to retrieve collagen type I, type III, elastin and fibronectin, the sections were incubated in Proteinase K (Sigma, St. Louis, MO) epitope retrieving solution for 30 min. at 37°C. The epitope retrieving solution was prepared by dissolving 20 $\mu\text{g}/\text{ml}$ Proteinase K (Sigma, St. Louis, MO) in a Tris-EDTA acid buffer (50mM Tris Base, 1mM EDTA) at pH 8.0. After epitope retrieval, the sections were incubated in a peroxidase suppressor (Pierce Biotechnology, Rockford, IL) for 30 min. to

quench any endogenous peroxidase activity, followed by incubation in a blocking buffer (Pierce Biotechnology, Rockford, IL) for 30 min. with serial washing in between, so as to suppress any non-specific binding of antibodies. The primary antibody was applied overnight at 4°C. After washing off the unbound primary antibody, a horseradish peroxidase (HRP)-conjugated secondary antibody was added and incubated at room temperature for two hours. The binding of the antibody was detected by adding metal enhanced diaminobenzidine (DAB) substrate (Pierce Biotechnology, Rockford, IL) to the sections and incubated for 1 to 3 min. to maximize the staining while preventing saturation.

For the examination of hyaluronic acid, biotinylated hyaluronic acid binding protein (HABP) (Calbiochem, San Diego, CA) which binds specifically and strongly to HA was used as the primary antibody. Unlike the other antibodies in Table 1, HABP reacts with both the HA synthesized by the host and those inherent in the acellular scaffold. The protocol for the visualization with HABP was also different from above, as no secondary antibody was required. After incubation with HABP overnight at 4°C, sections were washed and incubated with HRP-conjugated streptavidin (Calbiochem, San Diego, CA) for 40 min. The bound streptavidin label was located with DAB peroxidase substrate solution.

Epiglottic, tracheal tissues as well as the blood vessels in the larynx were used as positive controls because of the presence of collagen I and HA in epiglottic tissue, 15' 16 elastin and collagen III in blood vessels, 17 proteoglycans (PGs) and GAGs in cartilage cores, 18 and fibronectin in tracheal cartilage. 19 Laryngeal sections with the primary antibody replaced by negative serum were used as negative control.

Quantitative histological analysis

A Leica DM200 microscope (Bannockburn, IL) and a MicroFire microscope digital CCD camera (Optronics, Goleta, CA) were used to examine all the stained slides and to capture digital histological images.

The relative amounts or densities of collagen type I, type III, elastin, fibronectin, hyaluronic acid and glycosaminoglycans were estimated from their staining intensities and relative areas by digital image analysis using the NIH Image J software (Bethesda, MD). The procedure was modified from the principle described in Hammond et al. 20 and in Chan et al. 21 Briefly, color images were first converted to 8-bit grayscale images. The grayscale values for each image unit (pixel) in an image ranged from 0 to 255 with 0 (black) being minimum intensity and 255 (white) being maximum intensity. In order to compensate for the possible non-uniform illumination of an image in the Leica DM200 microscope, an 8-bit grayscale image of the illumination pattern was taken for a slide without any tissue specimen and was defined as the reference "background" image. All sample images were first normalized by dividing the grayscale values for all pixels by those of the background image, then multiplied by 255. 22' 23 For each grayscale image, visual comparisons were made with its corresponding H&E stained image, so as to select two threshold intensity values (a lower threshold and an upper threshold) such that pixels representing areas of a molecule of interest in the grayscale image can be clearly visualized with a minimum background intensity. Pixels with intensities within the two thresholds (between the lower and the upper thresholds) were deemed representative of the molecule of interest. For each larynx, the left (experimental) and the right (control) vocal folds were included in the same image so that the same threshold intensity values were always applied to both vocal folds, avoiding any bias in the image analysis procedure due to the use of different thresholds. The relative density of the protein of interest was then calculated as the fraction of the positively stained area to the total area of the implanted scaffold and the vocal fold tissues, including all soft tissues (i.e., thyroarytenoid (TA) muscles and connective tissues) but excluding the cartilaginous tissues and the supraglottic tissues.

The reliability of the manual image analysis procedure for the selection of thresholds and the areas of interest was examined. Two raters completed the image analysis of an identical vocal fold coronal section independently, each of them for 5 trials. The intra-rater reliability was determined as the percentage difference in relative protein densities from the 5 trials of analysis performed by the same rater, and the inter-rater reliability was determined as the percentage difference in relative protein densities between the two raters. Results showed that the mean percentage difference in relative protein densities (\pm standard deviation) obtained among the 5 trials completed by the same rater was $3.1471\% \pm 1.2304\%$ for one rater and $0.5320\% \pm 0.3617\%$ for the other. The mean percentage difference in relative protein densities among the trials completed by the two raters was $3.925\% \pm 2.7281\%$.

Statistical analysis

For the results of the quantitative digital image analysis, paired Student's *t* tests were conducted to determine if the expressions of the ECM proteins in the left vocal fold versus the right vocal fold (i.e., relative protein densities in the vocal fold implanted with the scaffold vs. those of control) were significantly different. The level of significance (α) was set at 0.05.

RESULTS

Coronal sections of the rat laryngeal specimens were obtained at a level approximately 1100 μm to 1350 μm posterior to the anterior commissure of the vocal folds, corresponding to the location of the acellular scaffold implants in the rat larynges. Figure 4 and Figures 5–8 show the typical histological images of the laryngeal specimens obtained at the various time points (3 days, 7 days, 30 days, and 90 days, respectively for Figs. 5–8) following implantation of the acellular scaffolds. The host response to the implanted scaffolds can be illustrated in the H&E images (Figs. 4, 5A, 6A, 7A, 8A). Figure 4 shows the H&E stained sections at high magnification (total magnification at up to 400 \times) for illustrating the implanted scaffolds and the host response they triggered in the vocal fold tissues, whereas Figs. 5A, 6A, 7A and 8A are at lower magnification to show all other laryngeal structures. Three days after the surgery (Figure 4A-1), inflammatory cells could be seen accumulating on the implant surface, with some infiltrating the bovine scaffold as well. According to the morphology, these inflammatory cells included lymphocytes, eosinophils, polymorphonuclear neutrophils (PMNs) and a few macrophages. In contrast, a smaller number of inflammatory cells was observed in the control wound. After 7 days, significant infiltration of inflammatory cells as well as a few fibroblasts could be observed in the implant (Figure 4B-2), whereas little cellular infiltration was observed in the control vocal fold. Thirty days following the surgery, the number of inflammatory cells around and in the implant decreased. Some small blood vessels and foreign body giant cells could be observed in the scaffold, yet no fibrotic tissue can be detected (Figure 4C-3). At the final time point (after three months), all scaffold implants could not be identified, having been apparently degraded or resorbed, with no evidence of calcification (Figure 4D). Also, no tissue necrosis was observed at any time point. Given that the wounds (of about 1.0 mm long and 0.5-2.0 mm deep) were created only in the cartilaginous vocal folds instead of in the membranous vocal folds that are prone to scarring, no scar tissue was found in the control vocal folds (Figs. 4A–D).

Figures 5, 6, 7, and 8 show the histological coronal sections of rat laryngeal specimens at lower magnification. Examination of type I collagen at different time points is shown in Figs. 5B, 6B, 7B and 8B, whereas type III collagen is shown in Figs. 5C, 6C, 7C and 8C. According to the manufacturer, the anti-type I collagen antibody could cross-react slightly with type III collagen, but not vice versa. In other words, although the anti-collagen I antibody could possibly stain collagen III, the anti-collagen III antibody was highly specific in labeling collagen III only. However, as the histological staining patterns (spatial

distributions) of collagen I and III associated with the anti-collagen I and the anti-collagen III antibodies were distinctly different from one another, the cross-reaction of type III collagen with the anti-collagen I antibody was deemed negligible for the rat collagen. In Figs. 5D, 6D, 7D, and 8D, the anti-elastin antibody heavily stained the mucosal area of the airway and the cartilaginous vocal folds, consistent with the findings of Tateya et al. 24 Comparing to the surrounding laryngeal connective tissues, the anti-fibronectin antibody stained the implanted scaffold intensely, as shown in Figs. 5E, 6E and 7E. By 90 days, the disappearance (apparent degradation) of the scaffold rendered similar staining pattern and intensity in both vocal folds (Fig. 8E). In Figs. 5F, 6F, 7F, and 8F, hyaluronic acid binding protein (HABP) was bound predominantly to the supraglottal tissue, as well as to the vocal fold muscle (thyroarytenoid muscle) and the implanted scaffold. Such staining pattern of HA with skeletal muscles agreed with a thorough analysis of the HA distribution in the body of the rat, 25 where HA was found in skeletal muscles in approximately 8% of the whole rat body, at a concentration of 132 fg/g. The results of Alcian blue staining (Figs. 5G, 6G, 7G and 8G) revealed glycosaminoglycans in the entire cartilaginous vocal fold throughout the 3 months, with the implanted scaffolds always staining more intensely than the surrounding laryngeal tissues.

The relative densities of key matrix proteins were estimated by quantitative digital image analysis of the histological sections subjected to immunohistochemistry (Figs. 5B–F, 6B–F, 7B–F, and 8B–F) and Alcian blue staining (Figs. 5G, 6G, 7G and 8G). Results of paired Student's *t* tests comparing the relative densities of proteins in the experimental vocal fold versus those in the control are shown in Table 2. Figure 9 shows the relative densities of collagen type I, collagen type III, elastin, fibronectin, hyaluronic acid and glycosaminoglycans in the experimental and the control vocal folds at the various time points. Results of the quantitative digital image analysis showed that the mean relative densities of matrix proteins in the vocal folds with the implanted scaffolds were almost always higher than those in the control vocal folds within three months post-surgery, with some differences in the acute wound healing stage being statistically significant (Figure 9). On day 3, the levels of collagen I and III in the implanted vocal folds were significantly higher than those in the control vocal fold (Figs. 9A, 9B). After 3 months, the levels of collagen I and III have gradually decreased to very close to those of the control. On day 3, the level of elastin was higher than that of the control with a marginally significant difference between the two (Table 2), followed by a gradual decrease over 3 months (Fig. 9C). Throughout the experimental period of 3 months, the mean relative densities of fibronectin, hyaluronic acid and GAGs in the experimental vocal folds with the scaffold implants were higher than those of the control at all time points (Figs. 9D, 9E, 9F), but statistically significant differences between the experimental and the control vocal folds were detected only for GAGs on day 3 (Fig. 9F).

DISCUSSION

This study introduced a novel methodology where a tissue engineering scaffold was successfully implanted into the rat vocal fold, without using the more surgically accessible method for delivering implants through injection (e.g., for hydrogels). Due to the small size of the rat vocal folds (around 1.5 to 2.0mm in length and less than 0.5mm in thickness of the lamina propria) and the difficulties in surgical delivery of the implant, in the present study the bovine acellular scaffolds were implanted into the more posterior, cartilaginous portion of the vocal fold to a depth of about 0.5 to 2.0 mm, instead of into the membranous vocal fold. Implantation of the scaffolds into the membranous vocal fold should be targeted for future studies in order to explore the potential of the acellular scaffold for reconstruction of the lamina propria. During the surgery, only a minimal amount of bleeding and swelling was observed (Fig. 1D), resulting in no detectable gross structural difference between the

experimental vocal fold (left) and the native vocal fold (right) 24 hours after surgery (Fig. 1E). Moreover, all 21 rats became active and started to eat and drink within 12 hours of the surgery, without any incidence of infection, behavioral abnormalities, or weight lost. These findings suggested that the surgical procedure and the scaffold implantation did not seem to introduce any adverse effects on the rats.

It was a promising finding for host fibroblasts to infiltrate the acellular scaffold implants, especially during the acute stage of wound repair as characterized by an inflammatory response and cellular proliferation. Unlike the typical host response to synthetic biomaterials, host fibroblasts could be seen readily attaching to the bovine acellular scaffold and eventually infiltrating a large portion of the implant, with no evidence of fibrotic capsule formation at any time point. These observations supported our previous studies on the pore architecture of the bovine acellular scaffold, which demonstrated that the scaffold has relatively high porosity (~90%) and intrinsic permeability (0.21 to 3.21 darcy), as well as optimal pore size and pore size distribution (>60% of the pores with equivalent diameters >10 μm) that could facilitate cellular attachment and infiltration. 7

In the present study, cells were only identified by their morphology. To further investigate the inflammatory reaction, foreign body reaction or even possible infection associated with the implantation, accurate identification and quantification of the cells using specific phenotypic markers should be pursued in future studies. In Figure 4, the appearance of lymphocytes in the scaffold implant and in surrounding tissues during the inflammatory response likely indicated the presence of some residual foreign epitopes in the scaffold. 26 Some degrees of adverse immune response to different kinds of acellular biological scaffolds, such as porcine small intestinal submucosa (SIS), have been widely reported and such response could be traced to the incomplete removal of cellular residuals. 27 New methods of decellularization to further minimize any possible adverse immune response should be explored in future studies. Furthermore, there was the possibility of infection, given that the surgery was conducted in the airway through the oral cavity. Since only 70% ethanol and UV light were used for sterilization in this study, more intensive, FDA approved sterilization procedures could be conducted in future studies to eliminate the possibility of infection. Yet typical sterilization for achieving clinical safety often includes harsh steps (such as oxidation and alkylation) that could have adverse effects on the structure and integrity of acellular ECM scaffolds. 28· 29 These possible adverse effects should be a direction for future studies as well.

Collagens and elastin are the major fibrous protein components of the vocal fold lamina propria. They are important ECM proteins for contributing to tissue geometry and viscoelasticity, as well as to the passive tensile stress generated during vocal fold length changes. 4· 21 Type I and type III collagens are the most dominant collagens in the vocal fold lamina propria, 15 with collagen I contributing to elasticity or stiffness of the tissue, and collagen III contributing to the ability to withstand dynamic stresses. 30 On the other hand, elastin contributes to the elastic recoil as well as stiffness of the vocal fold. In the present study, the mean relative densities of newly synthesized fibrous proteins (collagen I and III, and elastin) were found to be generally higher around the scaffold implants, suggestive of active ECM remodeling processes. In the vocal fold, scarring can be characterized by many factors including the density of collagen fibers, the degree of organization of the collagen deposit. 2 It is generally believed that highly organized collagen in fibrous bundles, especially collagen type I, is the basis of fibrosis and scar tissue formation. 2· 31 Hence, an accumulation of collagen induced by the implant is generally not favorable for constructive tissue remodeling. On days 3, the expressions of collagen type I and III in the experimental vocal fold were significantly higher than those in the control, whereas their expressions gradually decreased afterwards and became close to those of the control by 90 days. In

contrast, scarring in the rat membranous vocal fold has been associated with significant increases in the concentrations of collagen I and collagen III for up to 3 months post-surgery. 32 Furthermore, no fibrotic capsule was detected around the implant at every time point, implying that such active collagen synthesis in the acute wound healing stage was likely not inducing significant scarring during the tissue remodeling process over 3 months.

Fibronectin is abundantly found in regenerating or healing tissues. 33 It acts as a chemoattractant for fibroblasts and inflammatory cells such as monocytes during wound healing, which explains why a significant increase of fibronectin has been found in vocal fold scars, as well as in benign vocal fold lesions such as nodules and polyps. 32-34 Increase in fibronectin following injury is believed to be positive but only to an extent. When too much fibronectin is present, fibrosis may develop. 34 In the present study, the expressions of fibronectin in the vocal folds implanted with the acellular scaffold were at higher levels than the control, with marginally significant differences on day 3 and day 30. These changes were associated with the cellular migration and infiltration triggered by the scaffold and the wound healing process. As the scaffold was apparently degraded by 3 months, the fibronectin level dropped dramatically. This finding was consistent with previous results on wound healing of the rat vocal fold lamina propria, where significantly higher levels of fibronectin expressions were observed within one month post-surgery, with the process slowing down after 3 months. 32 Although the optimal fibronectin level needed for tissue repair has yet to be determined, the decrease in fibronectin along with the apparent degradation of the scaffold suggested that scar tissue formation was likely minimized.

Previous studies have shown that hyaluronic acid (HA) could facilitate wound healing in the vocal fold with minimal fibrosis and scarring. 35-36 It is also very important in maintaining the viscoelasticity of the vocal fold lamina propria 3-37 and in modulating the size and density of collagen fibers. 36 Nevertheless, an increase of HA could also indicate xenograft rejection, according to studies on mouse-to-rat cardiac xenografts. 38 According to the present data, despite the fact that HA was inherent in the acellular scaffold, the implantation induced no significant increase in the expressions of HA in the experimental vocal fold compared to the control, except a marginally significant increase on day 3 (Fig. 9E). A comparison of the histological images (Figs. 5F, 6F and 7F) showed that the level of HA within the scaffold decreased over time and became similar to that of the surrounding vocal fold tissue (TA muscle) within a month. Results of the quantitative image analysis also showed that HA in the experimental vocal fold decreased to a much lower level after 3 months (Fig. 9E). These findings suggested that the acellular scaffold xenograft was likely not rejected by the host.

Proteoglycans are ubiquitous molecules that have sophisticated and multifunctional roles, including such diverse functions as cell adhesion and migration, matrix assembly, binding and delivery of growth factors, immune functions, the binding of plasma proteins, as well as the modulation of wound healing. Diverse proteoglycans have been found in the vocal fold lamina propria and implicated in many normal and pathological processes. 3-33-36-39-40 The glycosaminoglycan (GAG) side chains of proteoglycans can be quantified by dye-binding methods using cationic dyes, such as Alcian blue which binds in proportion to the number of negative charges on the GAG chains. 13-14 In the present study, a significantly higher level of GAGs was detected for the scaffold implant on day 3, followed by a gradual decrease of the level of GAGs over 3 months. The significant difference of GAGs between the experimental and the control vocal folds on day 3 could be caused by the GAGs inherent in the bovine acellular scaffold, as the Alcian blue dye was not specific on the source of the GAGs. A gradual decrease in the total GAG content over time suggested that the degradation of inherent GAGs could be faster than the synthesis of new GAGs by the host fibroblasts in response to the scaffold.

Although some scaffold implants in some rats were positioned in slightly different locations in the vocal folds, e.g., some scaffolds were positioned more superiorly, close to the vocal fold surface, no evidence was found that any of the scaffolds were extruded. This was verified by the fact that all scaffold implants were clearly located histologically in the vocal folds up to 30 days after surgery, with significant infiltration of host cells. By 90 days, the scaffolds have apparently degraded, with no calcification nor fibrotic tissue observed in the histological sections, supporting the potential of the scaffold for constructive tissue reconstruction. Nonetheless, degradation of the implanted scaffold was not directly investigated in the present study as sensitive labeling techniques such as radioactive isotope tracing would be required. Moreover, the tissue remodeling and scaffold degradation processes between 1 month and 3 months were not investigated. These processes and the long-term response beyond 3 months should be among the directions for future studies.

CONCLUSIONS

This study reported the *in vivo* biocompatibility of a three-dimensional, biodegradable, acellular xenogeneic scaffold derived from the bovine vocal fold lamina propria in a rat model of vocal fold injury. The bovine acellular scaffold was implanted into surgically created vocal fold wounds in 20 rats, and the resulting *in vivo* host response and tissue remodeling processes were examined histologically. Results demonstrated significant cellular infiltration in the scaffold implant in the acute stage of wound repair (3 days and 7 days post-surgery). The mean relative densities of key matrix proteins in the implanted vocal folds were almost always higher than those in the control, especially in the acute stage of wound healing, indicating active extracellular matrix remodeling processes by the host fibroblasts. Although more accurate labeling and tracing techniques will be required for further investigation of the degradation process, histological results indicated that the implanted scaffolds have apparently degraded by 3 months, with no evidence of fibrosis or calcification. Another future direction is the modification of the degradation process, e.g., by using crosslinking reagents for modulation of the rate of degradation *in vivo*. Overall, these preliminary data supported the promise of the bovine acellular scaffold for bioengineering of the vocal fold *in vivo*. Further studies targeting the membranous vocal fold as well as involving a larger number of animals are required to verify the present findings pertaining to reconstruction of the vocal fold lamina propria. The long-term host response should be examined as well.

Acknowledgments

This work was supported by the National Institute on Deafness and Other Communication Disorders, NIH Grant No. 5 R01 DC006101-06. The authors would like to thank Jian Yang, Paula Timmons, Bao-Xi Qu, Hao Xu, Jinhui Shen, Ling Zou and the staff of the Animal Resource Center of UT Southwestern Medical Center for their assistance in various technical aspects of the experiments.

References

1. Ramig LO, Verdolini K. Treatment efficacy: voice disorders. *J Speech Lang Hear Res.* 1998; 41:S101–116. [PubMed: 9493749]
2. Hirano S. Current treatment of vocal fold scarring. *Curr Opin Otolaryngol Head Neck Surg.* 2005; 13:143–147. [PubMed: 15908810]
3. Gray SD, Titze IR, Chan RW, Hammond TH. Vocal fold proteoglycans and their influence on biomechanics. *Laryngoscope.* 1999; 109:845–854. [PubMed: 10369269]
4. Gray SD, Titze IR, Alipour F, Hammond TH. Biomechanical and histologic observations of vocal fold fibrous proteins. *Ann Otol Rhinol Laryngol.* 2000; 109:77–85. [PubMed: 10651418]
5. Sato K, Hirano M, Nakashima T. Stellate cells in the human vocal fold. *Ann Otol Rhinol Laryngol.* 2001; 110:319–325. [PubMed: 11307906]

6. Xu CC, Chan RW, Tirunagari N. A biodegradable, acellular xenogeneic scaffold for regeneration of the vocal fold lamina propria. *Tissue Eng.* 2007; 13:551–566. [PubMed: 17518602]
7. Xu CC, Chan RW. Pore architecture of a bovine acellular vocal fold scaffold. *Tissue Eng.* 2008 (in press).
8. Nowak, RM. Walker's mammals of the world. 6. Baltimore, MD: Johns Hopkins University Press; 1999. p. 1243-1714.
9. Tateya T, Tateya I, Sohn JH, Bless DM. Histological study of acute vocal fold injury in a rat model. *Ann Otol Rhinol Laryngol.* 2006; 115:285–292. [PubMed: 16676825]
10. Brudzynski SM. Principles of rat communication: quantitative parameters of ultrasonic calls in rats. *Behav Genet.* 2005; 35:85–92. [PubMed: 15674535]
11. Titze IR, Svec JG, Popolo PS. Vocal dose measures: quantifying accumulated vibration exposure in vocal fold tissues. *J Speech Lang Hear Res.* 2003; 46:919–932. [PubMed: 12959470]
12. Duprat Ade C, Costa HO, Lancelotti C, Ribeiro de Almeida R, Caron R. Histologic Behavior of the inflammatory process in autologous fat implantation in rabbit vocal folds. *Ann Otol Rhinol Laryngol.* 2004; 113:636–640. [PubMed: 15330143]
13. Bjornsson S. Simultaneous preparation and quantitation of proteoglycans by precipitation with alcian blue. *Anal Biochem.* 1993; 210:282–291. [PubMed: 8512063]
14. Moller, HJ.; Poulsen, JH. Staining of glycoproteins/proteoglycans in SDS-gels. In: Walker, J., editor. *Protein protocols handbook (Methods in molecular biology)*. Totowa: Human Press; 2002. p. 773-778.
15. Hahn MS, Teply BA, Stevens MM, Zeitels SM, Langer R. Collagen composite hydrogels for vocal fold lamina propria restoration. *Biomaterials.* 2006; 27:1104–1109. [PubMed: 16154633]
16. Hallen L, Johansson C, Laurent C, Dahlqvist A. Hyaluronan localization in the rabbit larynx. *Anat Rec.* 1996; 246:441–445. [PubMed: 8955783]
17. van der Rest M, Garrone R. Collagen family of proteins. *FASEB J.* 1991; 5:2814–2823. [PubMed: 1916105]
18. Madsen K, Lohmander S. Production of cartilage-typic proteoglycans in cultures of chondrocytes from elastic cartilage. *Arch Biochem Biophys.* 1979; 196:192–198. [PubMed: 507804]
19. Stechschulte DJ Jr, Wu JJ, Eyre DR. Fibronectin lacking the ED-B domain is a major structural component of tracheal cartilage. *J Biol Chem.* 1997; 272:4783–4786. [PubMed: 9030533]
20. Hammond TH, Gray SD, Butler JE. Age- and gender-related collagen distribution in human vocal folds. *Ann Otol Rhinol Laryngol.* 2000; 109:913–920. [PubMed: 11051431]
21. Chan RW, Fu M, Young L, Tirunagari N. Relative contributions of collagen and elastin to elasticity of the vocal fold under tension. *Ann Biomed Eng.* 2007; 35:1471–1483. [PubMed: 17453348]
22. Gonzales, RC.; Woods, RE. *Digital image processing.* 2. Singapore: Pearson Education; 2001. p. 567-642.
23. Rasband, WS. NIH Image J. US National Institutes of Health; Bethesda, MD: 1997–2007. <http://rsb.info.nih.gov/ij/>
24. Tateya T, Tateya I, Munoz-del-Rio A, Bless DM. Postnatal development of rat vocal folds. *Ann Otol Rhinol Laryngol.* 2006; 115:215–224. [PubMed: 16572612]
25. Reed RK, Lilja K, Laurent TC. Hyaluronan in the rat with special reference to the skin. *Acta Physiol Scand.* 1988; 134:405–411. [PubMed: 3227957]
26. Anderson, JM.; Cook, G.; Costerton, B.; Hanson, SR.; Hensten-Pettersen, A.; Jacobsen, N.; Johnson, RJ.; Mitchell, RN.; Pasmore, M.; Schoen, FJ.; Shirliff, M.; Stoodley, P. Host reactions to biomaterials and their evaluation. In: Ranter, BD.; Hoffman, AS.; Schoen, FJ.; Lemons, JE., editors. *Biomaterials science: An introduction to materials in medicine.* 2. London, UK: Elsevier Inc; 2004. p. 293-409.2004
27. Zheng MH, Chen J, Kirilak Y, Willers C, Xu J, Wood D. Porcine small intestine submucosa (SIS) is not an acellular collagenous matrix and contains porcine DNA: possible implications in human implantation. *J Biomed Mater Res B Appl Biomater.* 2005; 73:61–67. [PubMed: 15736287]

28. Hodde J, Janis A, Hiles M. Effects of sterilization on an extracellular matrix scaffold: part II. Bioactivity and matrix interaction. *J Mater Sci Mater Med.* 2007; 18:545–550. [PubMed: 17546413]
29. Hodde J, Janis A, Ernst D, Zopf D, Sherman D, Johnson C. Effects of sterilization on an extracellular matrix scaffold: part I. Composition and matrix architecture. *J Mater Sci Mater Med.* 2007; 18:537–543. [PubMed: 17546412]
30. Culav EM, Clark CH, Merrilees MJ. Connective tissues: matrix composition and its relevance to physical therapy. *Phys Ther.* 1999; 79:308–319. [PubMed: 10078774]
31. Ehrlich, HP. Collagen considerations in scarring and regenerative repair. In: Garg, HG.; Longaker, MT., editors. *Scarless wound healing.* New York: Marcel Dekker; 2000. p. 99-113.
32. Tateya T, Tateya I, Sohn JH, Bless DM. Histologic characterization of rat vocal fold scarring. *Ann Otol Rhinol Laryngol.* 2005; 114:183–191. [PubMed: 15825566]
33. Hirschi SD, Gray SD, Thibeault SL. Fibronectin: an interesting vocal fold protein. *J Voice.* 2002; 16:310–316. [PubMed: 12395983]
34. Thibeault SL, Bless DM, Gray SD. Interstitial protein alterations in rabbit vocal fold with scar. *J Voice.* 2003; 17:377–383. [PubMed: 14513960]
35. Thibeault SL, Rousseau B, Welham NV, Hirano S, Bless DM. Hyaluronan levels in acute vocal fold scar. *Laryngoscope.* 2004; 114:760–764. [PubMed: 15064637]
36. Ward PD, Thibeault SL, Gray SD. Hyaluronic acid: its role in voice. *J Voice.* 2002; 16:303–309. [PubMed: 12395982]
37. Chan RW, Gray SD, Titze IR. The importance of hyaluronic acid in vocal fold biomechanics. *Otolaryngol Head Neck Surg.* 2001; 124:607–614. [PubMed: 11391249]
38. Lorant T, Tufveson G, Johnsson C. The graft content of hyaluronan is increased during xenograft rejection. *Xenotransplantation.* 2004; 11:269–275. [PubMed: 15099207]
39. Pawlak AS, Hammond T, Hammond E, Gray SD. Immunocytochemical study of proteoglycans in vocal folds. *Ann Otol Rhinol Laryngol.* 1996; 105:6–11. [PubMed: 8546427]
40. Hahn MS, Kobler JB, Zeitels SM, Langer R. Midmembranous vocal fold lamina propria proteoglycans across selected species. *Ann Otol Rhinol Laryngol.* 2005; 114:451–462. [PubMed: 16042103]

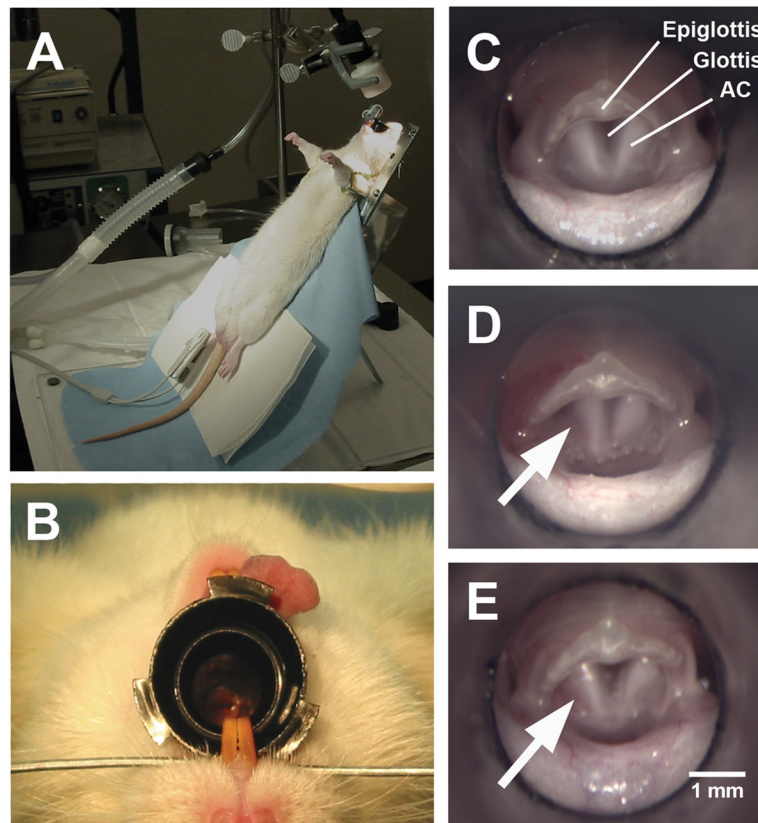


Figure 1.

Illustration of the surgical procedure for vocal fold implantation in the rat model. (A) A rat was secured on a customized surgical platform in supine position. (B) The rat larynx was visualized with a surgical microscope through a 4.0-mm otoscope specula. (C) Superior view of the rat larynx through the surgical microscope (top: anterior; bottom: posterior). (D) A wound was surgically created by a 1-mm long longitudinal incision on the superior surface of the left, posterior vocal fold (arrow) and two bovine acellular scaffold samples were implanted into the wound. No wound was created on the contralateral (right) vocal fold for this particular rat, but wounds were created on the right vocal fold as control in 20 rats. (E) 24 hours following surgery, the vocal fold implanted with the scaffolds (arrow) appeared normal (AC = arytenoid cartilage)

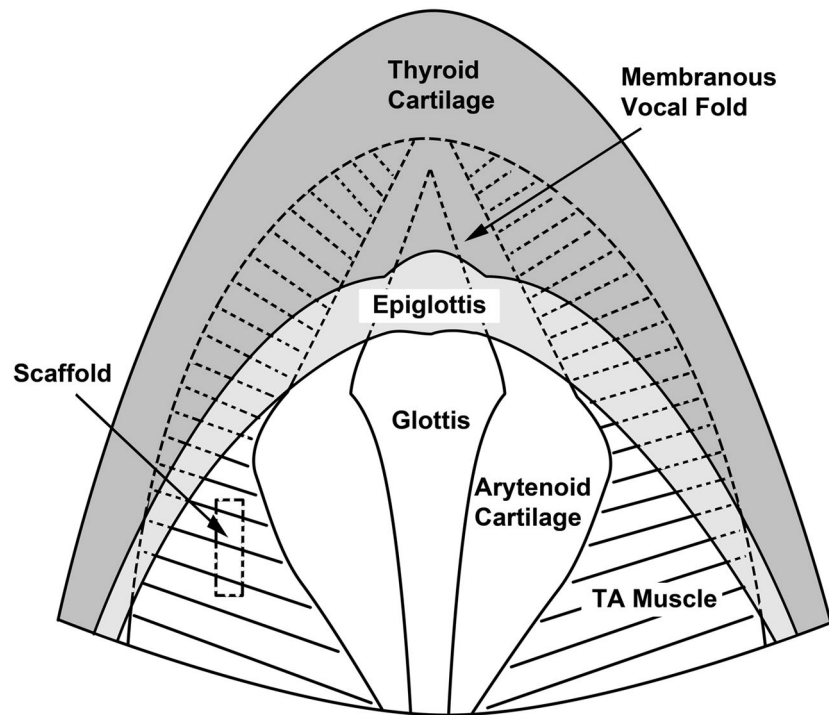


Figure 2. Schematic of the anatomy of the rat larynx as seen from a superior view similar to that of Figure 1C. The membranous vocal folds (shown in dotted lines) are obstructed by the epiglottis at this angle of view. The approximate location of an implanted scaffold is shown in the left cartilaginous vocal fold (TA = thyroarytenoid muscle).

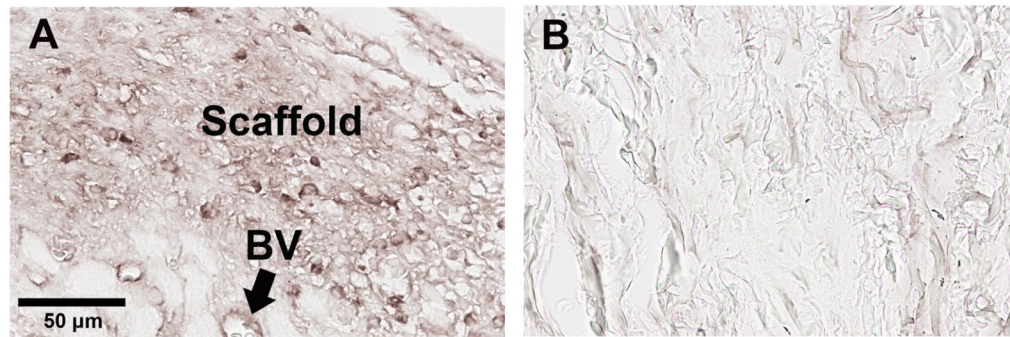


Figure 3. Immunohistochemical examination of fibronectin in (A) rat laryngeal coronal section; (B) bovine acellular scaffold section. The rat laryngeal specimen was harvested 30 days after the bovine scaffold implantation, showing the posterior vocal fold mucosa. The anti-rat fibronectin antibody reacts positively with the laryngeal mucosa integrated with the implanted scaffold in (A) (Left: medial; Right: lateral), whereas only background stain is observed for the bovine acellular scaffold in (B) (BV = blood vessels).

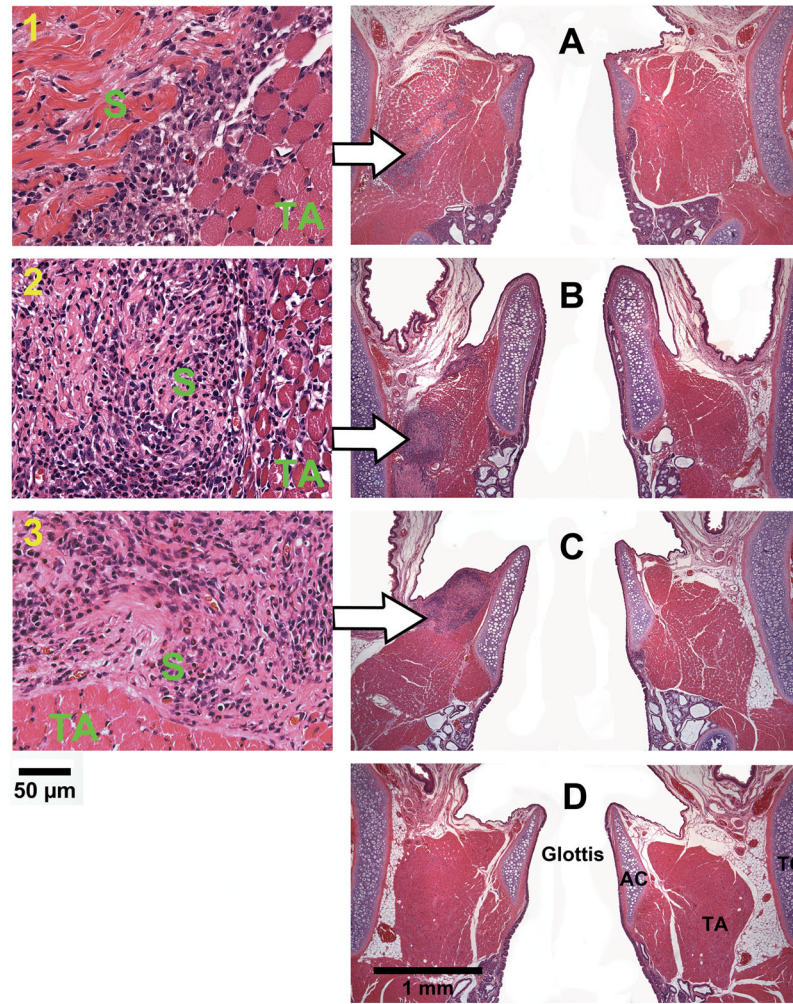


Figure 4. Histological coronal sections of rat laryngeal specimens stained with H&E, showing the acellular scaffolds implanted into the left vocal fold wounds (A) 3 days, (B) 7 days, (C) 30 days, and (D) 90 days after surgery (total magnification = 40×). Arrows indicate the implants in the left vocal folds (experimental vocal folds). Images on the left are at higher magnification (400×) showing the interface between the scaffold and the host tissue (1) 3 days, (2) 7 days, and (3) 30 days after surgery (AC = arytenoid cartilage; TA = thyroarytenoid muscle; TC = thyroid cartilage; S = implanted acellular scaffold).

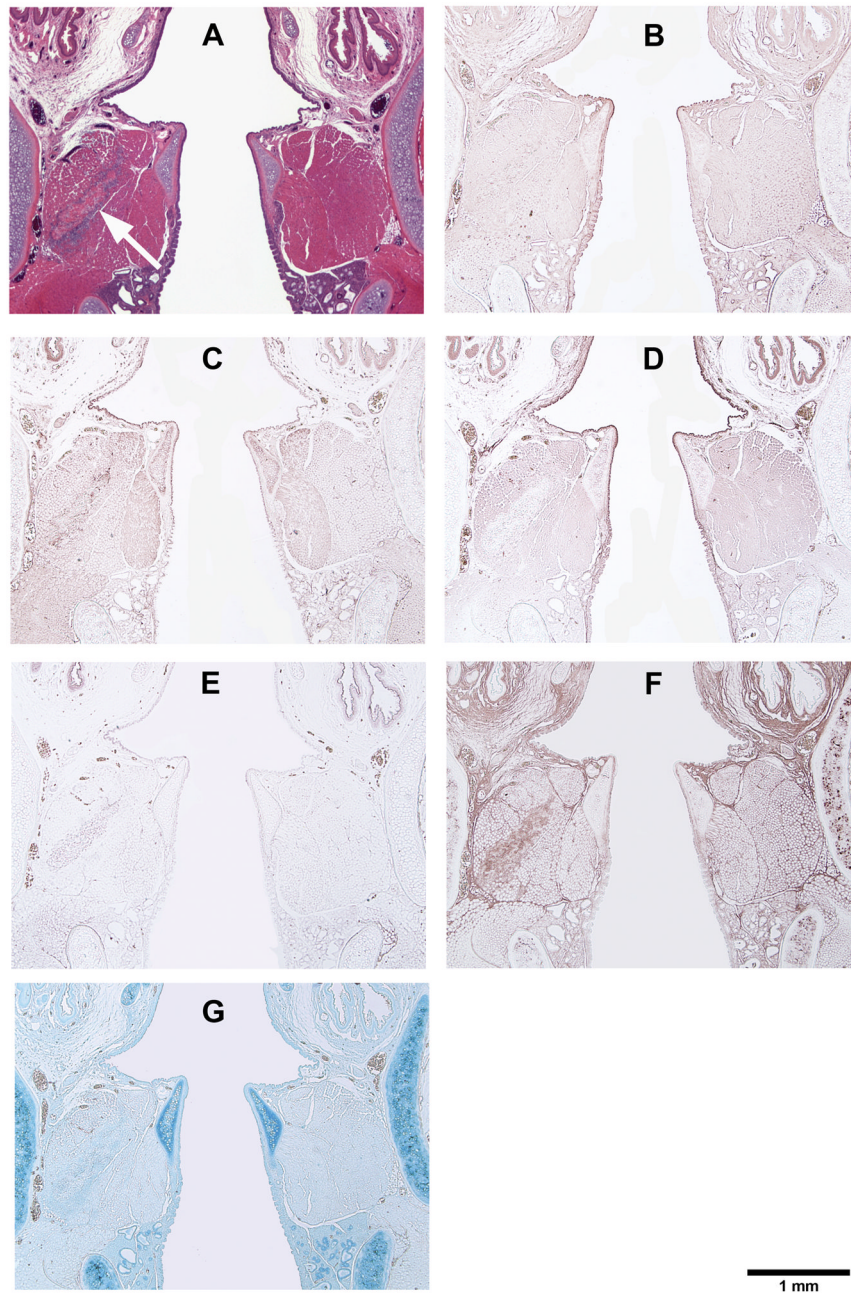


Figure 5. Histological coronal sections of rat laryngeal specimens showing the acellular scaffolds implanted into the left vocal fold wounds 3 days after surgery, with the right vocal fold wounds as control: (A) H&E (arrow indicates the implant in the left vocal fold); (B) Collagen type I; (C) Collagen type III; (D) Elastin; (E) Fibronectin; (F) Hyaluronic acid; (G) Glycosaminoglycans.

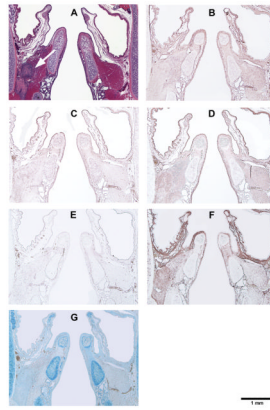


Figure 6. Histological coronal sections of rat laryngeal specimens showing the acellular scaffolds implanted into the left vocal fold wounds 7 days after surgery, with the right vocal fold wounds as control: (A) H&E (arrow indicates the implant in the left vocal fold); (B) Collagen type I; (C) Collagen type III; (D) Elastin; (E) Fibronectin; (F) Hyaluronic acid; (G) Glycosaminoglycans.

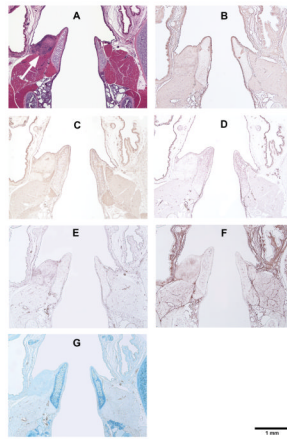


Figure 7. Histological coronal sections of rat laryngeal specimens showing the acellular scaffolds implanted into the left vocal fold wounds 30 days after surgery, with the right vocal fold wounds as control: (A) H&E (arrow indicates the implant in the left vocal fold); (B) Collagen type I; (C) Collagen type III; (D) Elastin; (E) Fibronectin; (F) Hyaluronic acid; (G) Glycosaminoglycans.

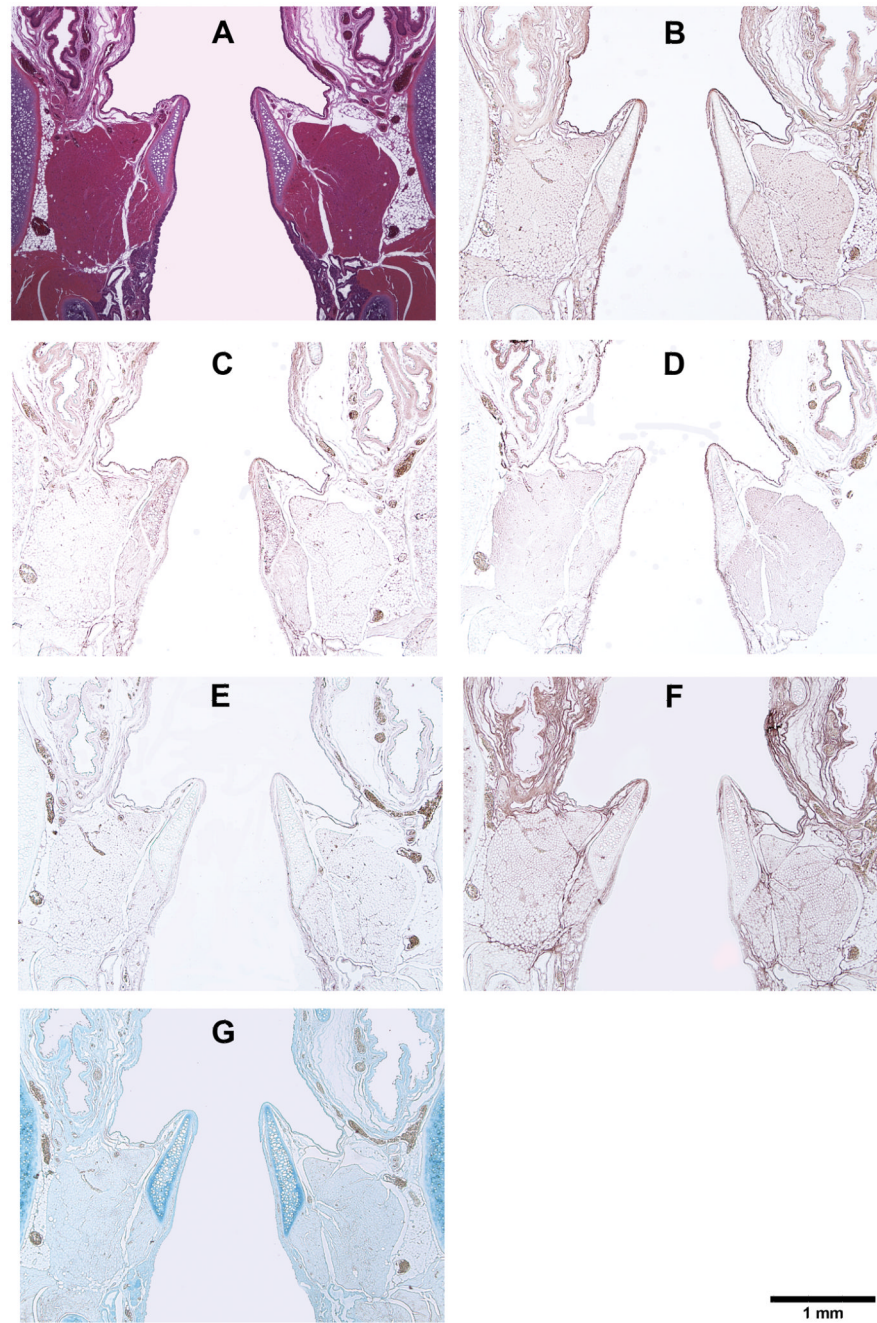


Figure 8. Histological coronal sections of rat laryngeal specimens showing the acellular scaffolds implanted into the left vocal fold wounds 90 days after surgery, with the right vocal fold wounds as control: (A) H&E (note the absence of the implant in the left vocal fold); (B) Collagen type I; (C) Collagen type III; (D) Elastin; (E) Fibronectin; (F) Hyaluronic acid; (G) Glycosaminoglycans.

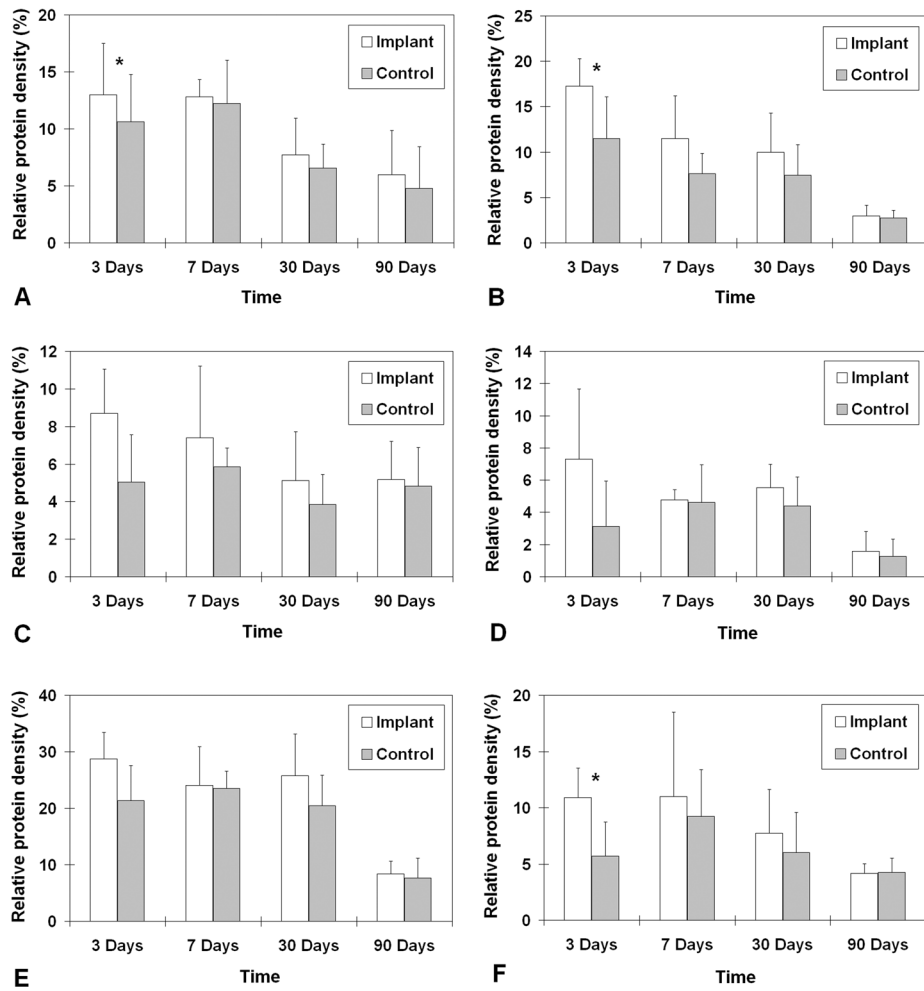


Figure 9. Relative densities of ECM proteins in the rat vocal fold implanted with the bovine acellular scaffold versus those in the control vocal fold (n = 5): (A) Collagen type I; (B) Collagen type III; (C) Elastin; (D) Fibronectin; (E) Hyaluronic acid; (F) Glycosaminoglycans. * $p < 0.05$ for differences between the implanted vocal fold and the control.

Table 1

List of the antibodies for immunohistochemistry

Antibody ^a	Immunogen or Clone	Vendor
Collagen type I	Type I collagen purified from fetal mouse skin	Calbiochem, San Diego, CA
Collagen type III	Type III collagen purified from fetal mouse skin, digested with cyanogen bromide	Calbiochem, San Diego, CA
Elastin	Elastin extracted and purified from rat aorta	Millipore, Billerica, MA
Fibronectin	Recombinant human fibronectin (Clone FBN11)	Calbiochem, San Diego, CA
Hyaluronic acid	Hyaluronic acid from bovine nasal cartilage (M.W. >= 2000)	Calbiochem, San Diego, CA

^a Epitope retrieval was achieved with Proteinase K, except for hyaluronic acid where biotinylated hyaluronic acid binding protein (HABP) was used.

Table 2

Results of paired Student's *t* tests (two-tailed; degrees of freedom = 4) on the relative densities of ECM protein components in the vocal fold implanted with the acellular scaffold versus those in the control vocal fold (n = 5).

Time after implantation	Collagen I	Collagen III	Elastin	Fibronectin	Hyaluronic acid	GAGs ^a
3 days	<i>t</i>	-4.59	-2.51	-2.76	-2.51	-4.52
	<i>p</i> value	0.007	0.010	0.066	0.051	0.011
7 days	<i>t</i>	-0.35	-1.88	-0.82	-0.20	-1.06
	<i>p</i> value	0.744	0.134	0.458	0.853	0.350
30 days	<i>t</i>	-1.02	-2.32	-2.53	-2.55	-1.13
	<i>p</i> value	0.365	0.081	0.065	0.063	0.320
90 days	<i>t</i>	-2.41	-1.34	-0.61	-1.90	0.27
	<i>p</i> value	0.074	0.252	0.577	0.130	0.798

^aGAGs = glycosaminoglycans